JOURNAL OF CATALYSIS **178,** 489–498 (1998)
ARTICLE NO. CA982163

Experimental and DFT Studies of Initiation Processes for Butane Isomerization over Sulfated-Zirconia Catalysts

Z. Hong,* K. B. Fogash,[1] R. M. Watwe,* B. Kim,† B. I. Masqueda-Jiménez,‡ M. A. Natal-Santiago,* J. M. Hill,* and J. A. Dumesic*,[2]

*Department of Chemical Engineering, University of Wisconsin, Madison, Wisconsin 53706; †Department of Chemical Engineering, State University of New York-Buffalo, Buffalo, NY 14260; and ‡Centro de Investigación y Estudios de Posgrado, FCQ, Universidad Autónoma de San Luis Potosí, México

Received December 8, 1997; revised May 18, 1998; accepted May 19, 1998

Reaction kinetics studies were conducted of isobutane and *n*-butane isomerization at 423 K over sulfated-zirconia, with the butane feeds purified of olefins. Dihydrogen evolution was observed during butane isomerization over fresh catalysts, as well as over catalysts selectively poisoned by preadsorbed ammonia. Butane isomerization over sulfated-zirconia can be viewed as a surface chain reaction comprised of initiation, propagation, and termination steps. The primary initiation step in the absence of feed olefins is considered to be the dehydrogenation of butane over sulfated-zirconia, generating butenes which adsorb onto acid sites to form protonated olefinic species associated with the conjugate base form of the acid sites. Quantum-chemical calculations, employing density-functional theory, suggest that the dissociative adsorption of dihydrogen, isobutylene hydrogenation, and dissociative adsorption of isobutane are feasible over the sulfated-zirconia cluster, and these reactions take place over Zr–O sites.

Key Words: **sulfated-zirconia; butane; isomerization; density-functional theory.**

INTRODUCTION

Catalysts based on sulfated-zirconia are active for the isomerization of *n*-butane at low temperatures, e.g., 300–423 K, and several authoritative reviews of this catalyst system have been compiled (1–7). In early studies, Holm and Bailey (8) reported that sulfate-treated zirconia-gel catalysts with or without Pt or Pd promoters were active for paraffin isomerization. Arata and co-workers (9, 10) reported that zirconia modified with sulfuric acid or ammonium sulfate was able to isomerize *n*-butane at low reaction temperatures. Hsu *et al.* (11) reported that sulfated-zirconia promoted with iron and manganese exhibited higher rates than sulfated-zirconia for *n*-butane isomerization at room temperature. More generally, sulfated-zirconia catalysts promoted with various metal components (e.g., W, Pt, Ni, and Fe) have been found to be effective for isomerization at low temperatures (11–21).

Because of the unique properties of sulfated-zirconia for butane isomerization, Arata and Hino (10) suggested that these materials might be superacidic. However, more recent studies by various research groups of the acid strength of sulfated-zirconia catalysts (17, 22–29) indicate that while these materials exhibit acid strengths similar to those of strong solid acids, e.g., H-Y zeolite, the acid strength of sulfated-zirconia is not unusually high. Moreover, assignment of superacidity based on observed catalytic activity may not be appropriate. For example, Sachtler and co-workers (17) found that while sulfated-zirconia promoted with Fe and Mn exhibited similar acid strength as unpromoted sulfated-zirconia, the promoted catalyst displayed higher catalytic activity for butane isomerization. In addition, Gates and co-workers (30, 31) determined that the presumed superacidity of promoted sulfated-zirconia did not extend to high temperature cracking reactions, and they suggested that low temperature isomerization may not be solely acid catalyzed.

Butane isomerization may be considered to be a surface chain reaction. There is general consensus that the propagation steps for butane isomerization at low temperatures are bi-molecular processes involving C_8 species (16, 32–40). The formation of the reactive intermediates that initiate these propagation steps may take place by several processes. For example, initiation of the surface chain reaction can occur by adsorption onto acid sites of olefins that are present in the feed or are produced by the catalyst (18, 35, 39, 41). The production of olefins by the catalyst may take place via dehydrogenation of butane (16–18, 35, 42–47). Alternatively, reactive intermediates may be generated by protolysis of butane (involving a carbonium ion species) over strong acid sites (48). Generation of reactive hydrocarbon radicals by the oxidation function of sulfated-zirconia

[1] Current address: Air Products and Chemicals, Inc., 7201 Hamilton Boulevard, Allentown, PA 18195-1501.

[2] to whom correspondence should be addressed

0021-9517/98 $25.00

catalysts may also be responsible for the initiation of butane isomerization (49).

In our previous research (39, 50), we observed that catalyst deactivation during isomerization of isobutane over sulfated-zirconia is much slower than deactivation during isomerization of *n*-butane. In the present paper we have taken advantage of this slower deactivation to investigate the initiation processes for isobutane isomerization over sulfated-zirconia. Importantly, we have observed the evolution of dihydrogen during isobutane isomerization over sulfated-zirconia, where olefins in the isobutane feed have been removed. In addition, we have conducted quantum-chemical calculations, employing density-functional theory, to study the feasibility of a dehydrogenation reaction as an initiation process over sulfated-zirconia catalysts.

EXPERIMENTAL

The sulfated-zirconia catalyst utilized in this study was provided by MEI (Flemington, NJ) in the form of a sulfated $Zr(OH)_4$ precursor, which was heated to 848 K in 1.5 h and maintained at this temperature for 2 h in 100 cm^3 (NTP)/min of dry O_2 per gram of precursor (where NTP designates 298 K and 1 atm). After activation, the catalyst was removed from the reactor, exposed to the atmosphere, and then stored in a desiccator. This catalyst had a BET surface area of 98 m^2/g and a sulfur loading of 1.8 wt% (Galbraith Laboratories).

Isobutane isomerization was carried out in a quartz flow-reactor (1.0 cm in diameter) loaded with 2.0 g of sulfated-zirconia. The catalyst was dried for 1 h at either 588 K (SZ-588) or 773 K (SZ-773) in 65 cm^3 (NTP)/min of flowing Ar (Liquid Carbonic). Reaction kinetics measurements were conducted over the catalyst at 423 K with 100% isobutane (Matheson, 99.0 wt% purity, C. P. grade) or 100% *n*-butane (AGA, 99.5 wt% purity, instrument grade). The total flow rate of feed to the catalyst was 65 cm^3 (NTP)/min. The olefin impurities in the isobutane feed, i.e., isobutylene and *n*-butenes, were removed via a trap of activated H-mordenite (3 g). Other impurities in the isobutane feed were *n*-butane (2200 ppm), propane (1900 ppm), and pentanes (less than 5 ppm) for which the kinetics data were corrected. The olefin impurities in the *n*-butane feed, i.e., mainly *n*-butenes, were also removed via the H-mordenite trap. Other impurities in the *n*-butane feed were isobutane (3700 ppm), propane (5500 ppm), and pentanes (less than 5 ppm) for which the kinetics data were corrected. Reaction products were analyzed using two gas chromatographs. A Hewlett Packard 5890 gas chromatograph with a thermal conductivity detector was employed to detect dihydrogen in the effluent, using a packed column (molecular sieve 13X, Alltech) held at 303 K for the separation of permanent gases, e.g., He, H_2, N_2, O_2, and CO. A Varian 3400CX gas chromatograph with a flame-ionization detector was employed for hydrocarbon analysis using a packed column (0.19% Picric Acid on Graphpac-GC, 80/100, Alltech) with temperature programming, i.e., column kept at 323 K for 5 min, then ramped to 373 K at a rate of 10 K/min, and kept at 373 K until the analysis was complete.

Reaction kinetics studies were also conducted using catalysts that were selectively poisoned by adsorbing ammonia, as described elsewhere (26). Briefly, the catalyst was first dried in flowing Ar (as described above), evacuated, and ammonia at an amount of 45 μmol/g was then dosed onto the sample at room temperature. The reactor was filled with Ar and the temperature was subsequently raised to 573 K for 1 h to achieve equilibration of ammonia on the catalyst. Reaction kinetics measurements were started after cooling the catalyst to 423 K.

COMPUTATIONAL METHODS

Density-functional theory (DFT) calculations were performed, using the hybrid, three-parameter functional B3LYP (51). This functional combines the exact HF exchange, Slater's local exchange functional, Becke's 1988 nonlocal gradient correction to the exchange functional, with the correlation functionals of Vosko–Wilk–Nusair (VWN) and Lee–Yang–Parr (LYP). These calculations were performed on DEC Alpha computers using the software packages Jaguar (52) and GAUSSIAN 94® (53). All the atoms except Zr were treated explicitly by using the 6-31G** basis set. For the Zr atom, the outermost core and valence electrons were treated explicitly, with the remaining core electrons treated with effective core potentials by using the basis set developed by Hay and Wadt (54). Reaction energetics predicted from the aforementioned methodology were not corrected by changes in zero-point energy to reduce the computational cost of our studies.

RESULTS

Experimental Results

Figure 1 shows the rates of dihydrogen production and *n*-butane production versus time-on-stream for isobutane isomerization at 423 K over sulfated-zirconia dried at 588 K (SZ-588) and over SZ-588 with 45 μmol/g of preadsorbed ammonia. For SZ-588, the initial rate of dihydrogen production (at 1 min time-on-stream) is about 5.2×10^{-3} μmol/(g • s). This rate subsequently decreases to 3.0×10^{-3} μmol/(g • s) after 3 min and then decreases gradually to 2.0×10^{-3} μmol/(g • s) for the next 70 min. The initial rate of *n*-butane production is about 1.45 μmol/(g • s), and this rate gradually decreases to 0.8 μmol/(g • s) for the next 70 min. As seen in Fig. 1, the rate of dihydrogen evolution correlates with the rate of isobutane isomerization. A similar

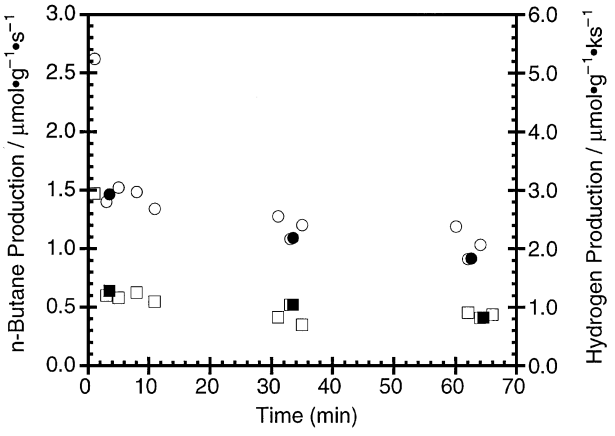

FIG. 1. Rates of dihydrogen production (open symbols) and *n*-butane production (filled symbols) at 423 K with 100% isobutane in feed over sulfated-zirconia versus time-on-stream: (●) *n*-butane production over SZ-588, on the left axis; (○) dihydrogen production over SZ-588, on right axis; (■) *n*-butane production over SZ-588 with 45 μmol/g of preadsorbed ammonia, on the left axis; (□) dihydrogen production over SZ-588 with 45 μmol/g of preadsorbed ammonia, on the right axis.

correlation between the rate of dihydrogen evolution and the rate of isomerization of isobutane was observed for isobutane isomerization at 423 K over the sulfated-zirconia catalyst dried at 773 K (SZ-773). In our previous studies (27, 28), it was observed that sulfated-zirconia dried at 773 K exhibits lower butane isomerization activity than sulfated-zirconia dried at 588 K. Accordingly, the rates of dihydrogen evolution and isobutane isomerization over the SZ-773 sample are both an order of magnitude lower than the corresponding rates over the SZ-588 sample.

Sulfated-zirconia (SZ-588) was selectively poisoned with preadsorbed ammonia (45 μmol/g of catalyst) to examine the effects of acidity on the rates of dihydrogen production and isobutane isomerization. As shown previously (26), selective ammonia adsorption in this manner poisoned the strongest acid sites on sulfated-zirconia (i.e., acid sites with heats of ammonia adsorption higher than 125 kJ/mol). Figure 1 shows that the rates of dihydrogen production and *n*-butane production for isobutane isomerization over the SZ-588 sample with preadsorbed ammonia are both about a factor of two lower compared to the corresponding rates over the SZ-588 sample. Importantly, the rate of dihydrogen production correlates with the rate of isobutane isomerization for the selectively poisoned sample.

Figure 2 shows the rates of dihydrogen production and isomerization versus time-on-stream for both isobutane isomerization and *n*-butane isomerization at 423 K over sulfated-zirconia dried at 588 K. Similar to isobutane isomerization, dihydrogen evolution was detected during *n*-butane isomerization over sulfated-zirconia. The initial rate of dihydrogen production (at 1 min time-on-stream) during isomerization of *n*-butane is about 2.7×10^{-3} μmol/(g • s); however, the rate decreases to the low level of 1.3×10^{-4} μmol/(g • s) after 3 min, and it remains at this low level for the next 70 min. The rate of isobutane production decreases more gradually from 2.05 μmol/(g • s) to 0.55 μmol/(g • s) within 70 min. Thus, the initial rate of dihydrogen production decreases rapidly within the first 3 min during *n*-butane isomerization, and therefore the rate of dihydrogen production during *n*-butane isomerization is an order of magnitude lower than the rate of dihydrogen production during isobutane isomerization for 3 to 70 min time-on-stream.

In addition to dihydrogen evolution, methane evolution was also observed during both isobutane isomerization and *n*-butane isomerization at 423 K over sulfated-zirconia (SZ-588). The rate of methane production is approximately equal to the rate of dihydrogen production for all time-on-stream during isobutane isomerization as well as during *n*-butane isomerization.

Quantum-Chemical Results

Various models for the structure of sulfate groups on sulfated-zirconia have been proposed in the literature (1, 17, 24, 55–59). These models were reviewed recently by Song and Sayari (6). As a feasibility study of the chemistry involved in the initiation process, a simplified representative structural model of sulfated-zirconia was used in quantum chemical calculations, as shown in structure I of Fig. 3. In this sulfated-zirconia cluster, the sulfate group is connected to the zirconium atom via two bridging oxygen atoms. The two coordinating oxygen atoms are terminated

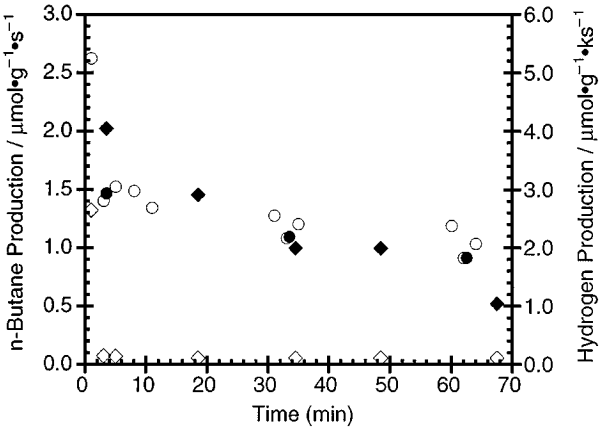

FIG. 2. Rates of dihydrogen production (open symbols) and butane isomerization (filled symbols) at 423 K with 100% butane in feed over sulfated-zirconia dried at 588 K: (●) *n*-butane production for isobutane isomerization, on the left axis; (○) dihydrogen production for isobutane isomerization, on the right axis; (◆) isobutane production for *n*-butane isomerization, on the left axis; (◇) dihydrogen production for *n*-butane isomerization, on the right axis.

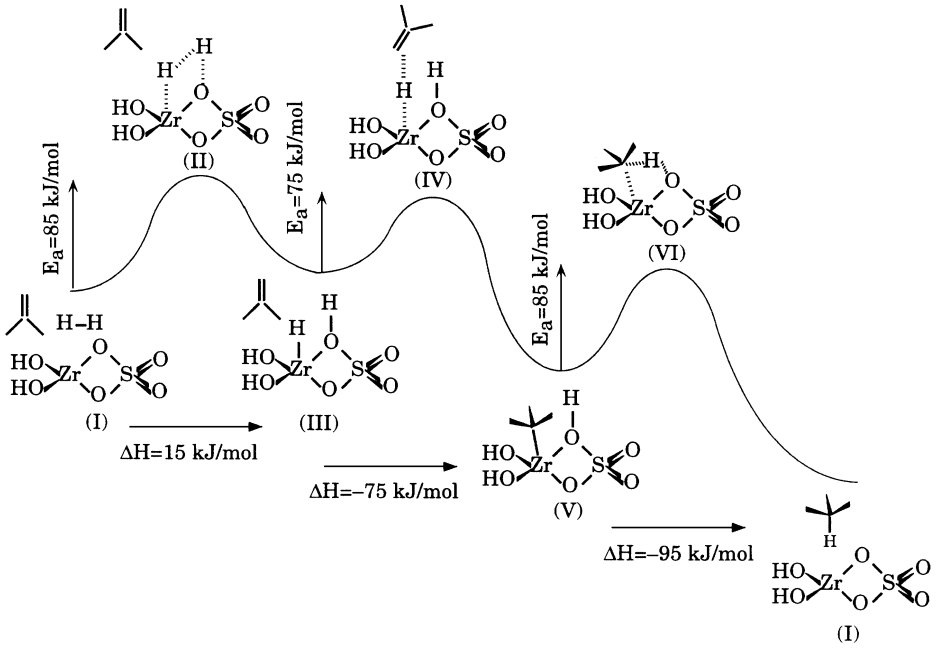

FIG. 3. Energy profile of a possible reaction pathway for dihydrogen dissociation and isobutylene hydrogenation over the sulfated-zirconia cluster.

by hydrogen atoms, in the form of hydroxyl groups, to maintain electrical neutrality for the entire cluster. The structure of this sulfated-zirconia cluster is similar to the model proposed by Tanabe and co-workers (2), and Yamaguchi (3). This model was chosen to represent the S–O–Zr site and the sulfate group which are the main features of numerous sulfated-zirconia models proposed. However, it should be noted that this model is only a simplified representative structure and it is used only for feasibility studies of possible initiation processes.

Figure 3 shows the calculated results of the energy profile of a possible reaction pathway for dihydrogen dissociation and isobutylene hydrogenation over the sulfated-zirconia cluster. Structural parameters were determined by optimizing to stationary points on the potential energy surface using internal coordinates. The clusters resulting from optimizations were classified as local minima or transition states on the energy surface by calculating the Hessian matrix numerically. For local minima, the eigenvalues of the Hessian matrix were all positive, whereas for transition states only one eigenvalue was negative. For these transition states, displacement along the eigenvector for the negative eigenvalue let to the reactant and product of the elementary step. As shown in Fig. 3, dihydrogen dissociation proceeds via a transition state (structure II) in which H–H interacts with the Zr–O site, to form a Zr–H bond and an O–H bond (structure III) over the sulfated-zirconia cluster. The calculated activation energy is ca. 85 kJ/mol for dihydrogen dissociation via this reaction pathway, and the calculated energy change associated with this mode of dihydrogen dissociation on the sulfated-zirconia cluster is ca. 15 kJ/mol. When isobutylene interacts with the dissociated hydrogen atoms on the sulfated-zirconia cluster, calculations show that this process proceeds through a transition state (structure IV) in which the methylene group of isobutylene attacks the hydrogen atom bonded to zirconium. This transition state leads to the formation of an isobutyl species bonded to the zirconium atom (structure V). The calculated activation energy of this process is ca. 75 kJ/mol, and the calculated energy change associated with this mode of isobutylene adsorption is ca. −75 kJ/mol. The adsorbed isobutyl species combines with the hydrogen atom bonded to the neighboring bridging oxygen to form isobutane. The hydrogen atom associated with the bridging oxygen interacts with the tertiary carbon in the isobutyl species, passing through a transition state (structure VI) with an activation energy of ca. 85 kJ/mol. This transition state leads to the formation and subsequent desorption of isobutane, and the associated energy change is ca. −95 kJ/mol.

Other possible reaction pathways of dihydrogen dissociation over this sulfated-zirconia cluster were also examined, e.g., dihydrogen activation over the S=O site in the sulfate group. The calculated activation energies of the transition states for various modes of dihydrogen adsorption on the sulfated-zirconia cluster are listed in Table 1. As shown in Table 1, the activation energies for dihydrogen dissociation are much higher for interactions with a S=O site compared to the aforementioned Zr–O site. These high activation energies of dihydrogen dissociation over a S=O site suggest that the activation of dihydrogen or isobutane over the Zr–O site is the most feasible pathway for dissociative adsorption.

TABLE 1

Activation Energies of Various Modes of Dihydrogen Dissociation over the Sulfated-Zirconia Cluster

Interaction site for dihydrogen dissociation	Structural model of transition state	Activation energy (kJ/mol)
Zr–O	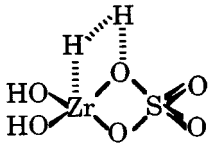	85
O in S=O	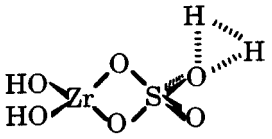	315
S=O	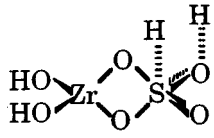	285

DISCUSSION

Surface Chain Reaction

Figure 4 shows a simplified reaction scheme for isobutane isomerization over sulfated-zirconia at 423 K. This scheme can be viewed as a surface chain reaction comprised of initiation, propagation, and termination steps. As mentioned earlier, the surface chain reaction can be initiated via several pathways as shown in Fig. 4. The propagation steps involve oligomerization of C_4 species to form C_8 species, rearrangement, and ß-scission of C_8 species, and hydride transfer from gas phase isobutane to the reactive intermediates, leading to isomerization products and isobutyl reactive intermediates. The termination steps involve coke formation, as well as hydride transfer between isobutane and higher molecular weight reactive intermediates to form, for example, C_6 and C_8 alkanes.

Propagation Steps

Based on carbenium ion chemistry in solution, the isomerization of butane can proceed via two reaction pathways, i.e., mono-molecular and bi-molecular processes (17, 32, 33, 60–62). The mono-molecular mechanism involves the formation of a primary carbenium ion, which is energetically unfavorable compared to a secondary carbenium ion. In the bi-molecular mechanism, as proposed by Guisnet and co-workers (33, 34), two C_4 species interact to form a C_8 intermediate, and the C_8 intermediate undergoes rearrangements and ß-scission to form isomerized C_4 species, or C_3 and C_5 species. Importantly, the bi-molecular mechanism does not proceed through a primary carbenium ion. With evidence from isotopic scrambling experiments, Sachtler and co-workers (16, 35) showed that the bi-molecular mechanism was the dominant reaction pathway for the isomerization of *n*-butane over Fe-Mn promoted sulfated-zirconia and unpromoted sulfated-zirconia catalysts. Gates and co-workers (36–38) also suggested a bi-molecular pathway for *n*-butane and isobutane isomerization over Fe- and Mn-promoted sulfated-zirconia. In

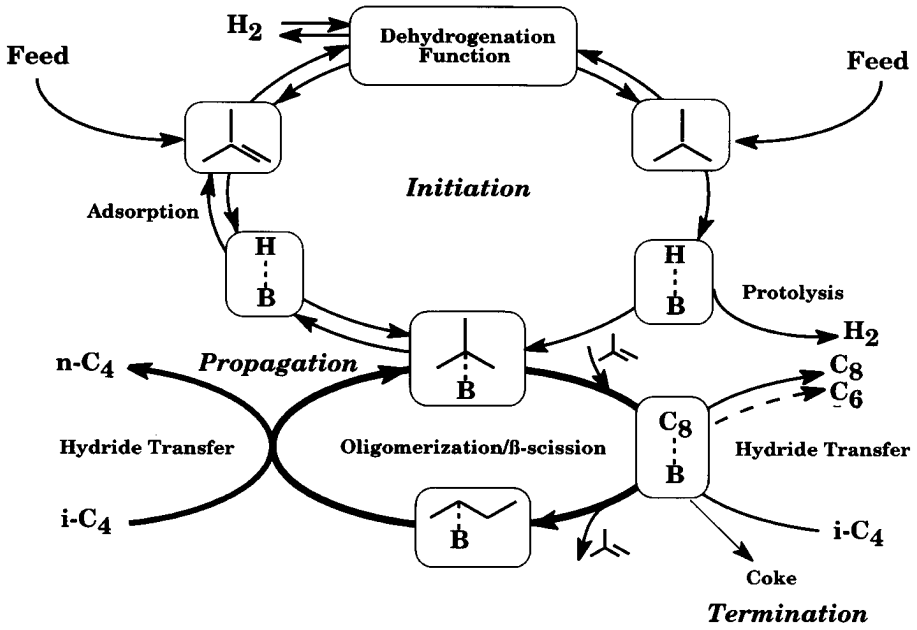

FIG. 4. Surface chain reaction scheme for isobutane isomerization over sulfated-zirconia.

agreement with the bi-molecular mechanism, our reaction kinetics studies (39) suggested that the isomerization reaction pathway proceeds via a C_8 intermediate which can undergo isomerization and ß-scission to produce *n*-butane or isobutane as well as the observed disproportionation products (C_3 and C_5 species). Recently, Guisnet and co-workers (40) suggested that dihydrogen inhibited the bi-molecular mechanism and higher temperatures favored the monomolecular pathway. Finally, the propagation steps are completed by hydride transfer from isobutane to the *n*-butyl species formed via oligomerization/ß-scission steps, to produce *n*-butane and adsorbed isobutyl species.

Initiation Steps

Initiation may occur via adsorption of olefins present in the feed stream onto acid sites. Sachtler and co-workers (18, 35) proposed that the isomerization reaction was initiated by small amounts of olefins, either in the feed or produced by the catalyst. A decrease in the level of olefins fed to the catalyst resulted in lower catalytic activity accompanied by slower catalyst deactivation (18, 39, 50). Davis and co-workers (41) reported promotional effects of olefins on the catalytic activity for butane isomerization over promoted sulfated-zirconia.

Clearly, the presence of olefins in the feed affects the reaction behavior; however, it is still unclear whether the presence of olefins in the feed is required for catalytic activity over sulfated-zirconia. For example, Davis and co-workers (63) reported that olefins in the feed are necessary for butane isomerization at low temperatures over sulfated-zirconia with their pretreatment conditions. However, as shown in Figs. 1 and 2, for our pretreatment conditions of the sample we have found that sulfated-zirconia is still active for butane isomerization at 423 K, even without detectable levels of olefins present in the feed (39, 50). This observation suggests that sulfated-zirconia is able to generate reactive intermediates *in situ* to initiate the surface chain reaction.

One process to generate reactive intermediates involves *in situ* dehydrogenation of isobutane to form dihydrogen and isobutylene. The isobutylene can then adsorb onto acid sites to form reactive intermediates. Sachtler and co-workers (18) have suggested that unpromoted sulfated-zirconia is able to produce butene from butane. Importantly, as shown in Fig. 1, we have detected the evolution of dihydrogen during isobutane isomerization over sulfated-zirconia at 423 K in the absence of feed olefins. In addition, the production of dihydrogen correlates with the observed catalytic activity for isobutane isomerization (see Fig. 1). It should be noted that C_4 olefins were not detected in the effluent during isobutane isomerization over sulfated-zirconia, suggesting that olefins produced in the dehydrogenation process undergo further reactions over the catalyst. In fact, the promotional effects of the addition of Pt or Fe-Mn to sulfated-zirconia may be related to the dehydrogenation activity of the additive (16, 18, 35, 45, 61).

The generation of reactive intermediates by sulfated-zirconia may also occur via a redox process. Farcasiu and co-workers (49, 64–66) proposed that sulfated-zirconia is a bi-functional catalyst, which possesses both strong acidity and oxidative properties. These authors suggested that alkane reactions over sulfated-zirconia might be initiated through a one-electron oxidation of the alkane by sulfate species to produce a carbocation precursor. Riemer and Knözinger (42) suggested that sulfated-zirconia possesses oxidizing properties in addition to strong acidity, based on the detection of oxidized phosphorous species on the surface of sulfated-zirconia following exposure of the catalyst to trimethylphosphene. Ng *et al.* (67) suggested that sulfate species are reduced during *n*-butane isomerization over sulfated-zirconia by *n*-butane or by hydrogen generated *in situ*. Sachtler and co-workers (43) showed that sulfate groups were reduced on sulfated-zirconia in the presence of dihydrogen. TPD studies (68) and TPR studies (44) of sulfated-zirconia catalysts also indicate that the sulfate groups can be reduced. For example, TPD studies of benzene adsorbed on promoted sulfated-zirconia indicate the presence of oxidized species on the surface (45–47). Adeeva *et al.* (17) detected the presence of sites capable of oxidizing acetonitrile on sulfated-zirconia and Fe- and Mn-promoted sulfated-zirconia.

It is also possible to form reactive intermediates via protolysis of isobutane. Gates and co-workers (48) proposed that initiation processes over sulfated-zirconia-based catalysts occur when the alkane is protonated by an acid site, forming a carbonium ion species (or transition state) which decomposes to generate a reactive hydrocarbon intermediate (i.e., a protonated olefin associated with the conjugate base form of the acid site) and dihydrogen or methane. As proposed previously by Olah (69), this reaction pathway requires extremely strong acidity. However, results from recent studies suggest that sulfated-zirconia catalysts exhibit acid strength similar to strong solid acids, e.g., H-mordenite, which are not generally considered to be superacidic (17, 22–28). Furthermore, in the absence of feed olefins, H-mordenite is not active for isobutane isomerization at 473 K (70). Therefore, it appears that isobutane at low temperatures cannot be activated via protolysis by an acid site on H-mordenite or by an acid site with acid strength similar to H-mordenite. Thus, as suggested by Gates and co-workers (30, 31), the low temperature isomerization of butane may not be solely acid catalyzed.

In the present study, selective poisoning with ammonia of the strongest acid sites on sulfated-zirconia does not eliminate catalytic activity (see Fig. 1), although the rates of hydrocarbon production and dihydrogen production are suppressed. In particular, dihydrogen evolution was still observed even though the strongest acid sites of

sulfated-zirconia were poisoned by preadsorbed ammonia (see Fig. 1). This result suggests that protonation of isobutane by the strongest acid sites is not the primary mode for initiation of isobutane isomerization.

As reported in the literature (18, 20), the presence of dihydrogen in the feed decreases the rate of butane isomerization over sulfated-zirconia. Chemisorption measurements for dihydrogen on the SZ-588 sample at 423 K show little uptake. Thus, the suppression of butane isomerization by dihydrogen may not be caused by the competitive adsorption of dihydrogen on the acid sites; i.e., dihydrogen does not block the acid sites. Rather, it appears that dihydrogen in the feed may inhibit isomerization by shifting the equilibrium for isobutane dehydrogenation, thereby limiting the rate of initiation.

As shown in Fig. 2, there are clear differences in the rates of dihydrogen evolution during isobutane and *n*-butane isomerization. Experimental studies by Olah *et al.* (71) of the protolysis of straight and branched paraffins in liquid superacidic solutions indicate that protolysis of isobutane produces both dihydrogen and methane, while protolysis of *n*-butane produces primarily methane. In our studies of *n*-butane isomerization over sulfated-zirconia, we observed production of dihydrogen, although at lower levels than during isobutane isomerization, and the rate of dihydrogen production decreased faster than during isobutane isomerization (see Fig. 2). Furthermore, the rate of methane production was approximately equal to the rate of dihydrogen production during the isomerization of isobutane as well as during the isomerization of *n*-butane. This observation suggests that the production of dihydrogen and methane does not take place via protolysis of butane, since the production of dihydrogen would not be expected from the protolysis of *n*-butane. Accordingly, it is possible that the production of dihydrogen takes place via a dehydrogenation pathway in which there is no preference in the dehydrogenation of isobutane versus *n*-butane, rather than via protolysis where methane evolution is favored over dihydrogen evolution for *n*-butane cleavage.

It is possible that dihydrogen could also be produced by deposition of coke on the catalyst. However, we have observed that the rate of dihydrogen production during isomerization of *n*-butane is lower than during isomerization of isobutane, while the rate of catalyst deactivation caused by coke formation is actually faster during isomerization of *n*-butane. Therefore, we suggest that dihydrogen is produced primarily in the initiation step involving dehydrogenation of isobutane.

Termination Steps

Termination of the surface chain reaction may occur via coke formation and hydride transfer from isobutane to higher molecular weight species on the catalyst. In this respect, we have observed production of higher molecular weight paraffins, e.g., C_6 paraffins, during isobutane isomerization and *n*-butane isomerization (50). We observed that the rates of production of these higher molecular weight paraffins during isobutane isomerization are higher than during *n*-butane isomerization (50). Furthermore, when C_4 olefins were present in the feed during isobutane isomerization, no C_4 olefins were detected in the effluent (50). It appears that during isobutane isomerization, sulfated-zirconia can effectively consume feed olefins via oligomerization processes to form higher molecular weight species followed by hydride transfer from isobutane to produce higher molecular weight paraffins. In contrast to this situation for isobutane isomerization, C_4 olefins were eventually detected in the reactor effluent when C_4 olefins were present in the feed during *n*-butane isomerization (50). Thus, sulfated-zirconia does not consume feed olefins as effectively during *n*-butane isomerization as during isobutane isomerization, mostly likely because of slower hydride transfer from *n*-butane to higher molecular weight species on the catalyst surface. According to Brouwer (72, 73), hydride abstraction from isobutane is more favorable than hydride abstraction from *n*-butane.

The different rates of the termination steps during isobutane and *n*-butane isomerization may explain the different rates of dihydrogen production (see Fig. 2). Slower hydride transfer during *n*-butane isomerization than during isobutane isomerization may result in the accumulation of olefinic surface species, which may lead to the formation of coke on the surface and block the catalytic sites. The more extensive coke formation and inhibition of the catalytic sites may be responsible for the faster catalyst deactivation as well as lower rates of dihydrogen production during *n*-butane isomerization than during isobutane isomerization.

It appears that the drying temperature employed during catalyst pretreatment affects the rates of both dihydrogen and hydrocarbon production, as discussed above. Thus, the observation by Davis and co-workers (63) that olefins in the feed are necessary for butane isomerization over sulfated-zirconia at low temperatures might be caused by slower rates of initiation on a more dehydroxylated surface (i.e., dried at 773 K).

Feasibility of Dehydrogenation of Isobutane

Figure 3 shows the reaction pathway of H_2 dissociation and isobutylene hydrogenation over a representative sulfated-zirconia cluster. According to our quantum-chemical calculations, H_2 may dissociate over the Zr–O site, and the activation energy of this step (ca. 85 kJ/mol) suggests that this process is feasible at our reaction conditions. Domen and co-workers (74, 75) reported that H_2 dissociates heterolytically on ZrO_2 at room temperature, giving IR-active bands at 3668 and 1562 cm^{-1} from O–H and Zr–H stretching modes, respectively. Although other types of H_2 adsorption are also possible, e.g., associative adsorption

and homolytic dissociative adsorption, the predominant form of H_2 adsorption on ZrO_2 at temperatures above 223 K is heterolytic dissociative adsorption. The activation energy for this mode of adsorption was estimated to be ca. 40 kJ/mol from infrared spectroscopic measurements, and this result is in general agreement with our calculations. Moreover, theoretical studies of H_2 dissociative adsorption on a ZrO_2 surface by Nakatsuji *et al.* (76) showed that the calculated activation energy for heterolytic dissociation of H_2 was ca. 90 kJ/mol, and the heat of dissociative adsorption was exothermic by ca. 95 kJ/mol relative to gaseous H_2. Our results give an activation energy for H_2 dissociative adsorption over the sulfated-zirconia cluster similar to the value calculated by Nakatsuji *et al.* (76) for H_2 dissociative adsorption over zirconia. The adsorption heats were different from these calculations, probably because of different clusters used in the calculations.

Based on our calculations, one possible pathway for isobutylene hydrogenation is that isobutylene may interact with the hydrogen atom bonded to zirconium to form an isobutyl species associated with zirconium, and this isobutyl species may further combine with a hydrogen atom attached to neighboring oxygen to form isobutane. Our calculated activation energies are ca. 75 kJ/mol for the first step and ca. 85 kJ/mol for the second step, suggesting that this reaction pathway is feasible at our reaction conditions. This pathway implies that isobutylene hydrogenation may proceed over a Zr–O site. A similar reaction pathway was proposed by Kokes *et al.* (77) for ethylene hydrogenation over zinc oxide, where H_2 dissociative adsorption is activated over a Zn–O site to form Zn–H and O–H species with an activation energy even lower than that over a Zr–O site. Domen *et al.* (78) reported that ethylene did not react with preadsorbed ZrH and ZrOH species at temperatures near 223 K. However, this reaction temperature is much lower than our reaction temperature (423 K).

Following the reverse direction of Fig. 3, isobutane may undergo dissociative adsorption over a Zr–O site to form an isobutyl species associated with Zr and a H species associated with the neighboring bridging oxygen atom. The isobutyl species may participate in initiation reactions of the acid-catalyzed butane isomerization over sulfated-zirconia by desorbing from Zr to form isobutylene and ZrH, or by migrating onto acid sites to form reactive intermediates in the acid-catalyzed surface chain reaction. The hydrogen atoms in the forms of Zr–H and O–H may combine to form dihydrogen molecules. It should be noted that isobutylene was not detected during the isobutane isomerization over sulfated-zirconia catalysts. This observation suggests that isobutylene, once formed, undergoes further reactions, e.g., involved in the initiation of the surface chain reaction and in the oligomerization reactions.

We have shown in earlier work that the rate of butane isomerization over sulfated-zirconia catalysts is sensitive to the hydration state of the catalyst (27, 28, 79). González *et al.* (27, 28) showed that the catalytic activity of sulfated-zirconia catalysts dried at 773 K could be increased by addition of ca. 70 μmol/g of water, and infrared spectra of this catalyst showed that the primary effect of this water addition was to increase the extent of hydrogen bonding on the surface. Thus, it is possible that the promotional effect is related to stabilization of the reactive intermediates by hydrogen bonding with the hydroxyl groups. The stabilization from hydrogen bonding may also facilitate the surface migration of isobutyl species from zirconium atoms to acid sites, thereby increasing the rate of isobutane dehydrogenation. Indeed, we observed a higher rate of dihydrogen production during isobutane isomerization over SZ-588 than over SZ-773.

In short, based on our quantum-chemical studies, a possible reaction pathway for dihydrogen dissociation, isobutylene hydrogenation, and isobutane dissociation over the sulfated-zirconia cluster is proposed, and the calculated activation energies suggest that this pathway is feasible at reaction conditions employed for butane isomerization (e.g., 423 K). These reactions may take place over the Zr–O site in the sulfated-zirconia cluster. The dehydrogenation of isobutane may be responsible for initiation process during butane isomerization over sulfated-zirconia, whereas dihydrogen dissociative adsorption and hydrogenation of isobutylene may be responsible for the inhibiting effect of H_2 on the rate of isomerization over sulfated-zirconia catalysts. It appears that the sulfate group does not participate directly in the initiation process of isobutane activation. However, the acid sites created by the sulfate groups on the catalyst are responsible primarily for the propagation steps in the surface chain reaction.

CONCLUSIONS

Butane isomerization at 423 K over sulfated-zirconia can be viewed as being a surface chain reaction comprised of initiation, propagation, and termination steps. The surface chain reaction can be initiated, for example, by adsorption of olefins present in the feed stream onto acid sites to form protonated olefins associated with the conjugate base form of the acid sites. Importantly, sulfated-zirconia is active for butane isomerization at 423 K without olefins present in the feed, indicating that sulfated-zirconia is able to generate olefins or reactive intermediates *in situ* to initiate the surface chain reaction. These olefins or reactive intermediates can be generated on sulfated-zirconia by dehydrogenation of butanes, by oxidation of butanes, or by protolysis of butanes over strong acid sites.

Experimental evidence for the generation of olefins by sulfated-zirconia was provided by detecting the production of dihydrogen during butane isomerization. The rate of dihydrogen production correlates with the rate of isobutane

isomerization. Though the activation of isobutane over sulfated-zirconia may proceed via protolysis on strong acid sites, dihydrogen evolution during isobutane isomerization was still observed over sulfated-zirconia catalysts that have been selectively poisoned by preadsorbed ammonia. Thus, protolysis of isobutane by strong acid sites does not appear to be the primary mode for initiation for butane isomerization over sulfated-zirconia. Instead, it appears that the initiation of butane isomerization over sulfated-zirconia takes place via a dehydrogenation process. The results of quantum-chemical calculations suggest that hydrogenation/dehydrogenation processes over sulfated-zirconia are feasible, and the reaction pathways for dihydrogen dissociation, isobutylene adsorption, and isobutane formation may take place over Zr–O sites.

ACKNOWLEDGMENT

We wish to acknowledge funding for this work from the Office of Basic Energy Sciences of the U.S. Department of Energy.

REFERENCES

1. Arata, K., *Adv. Catal.* **37**, 165 (1990).
2. Tanabe, K., Hattori, H., and Yamaguchi, T., *Crit. Rev. Surf. Chem.* **1**, 1 (1990).
3. Yamaguchi, T., *Appl. Catal.* **61**, 1 (1990).
4. Corma, A., *Chem. Rev.* **95**, 559 (1995).
5. Davis, B. H., Keogh, R. A., and Srinivasan, R., *Catal. Today* **20**, 219 (1994).
6. Song, X., and Sayari, A., *Catal. Rev. - Sic. Eng.* **38**, 329 (1996).
7. Adeeva, V., Liu, H. Y., Xu, B. Q., and Sachtler, W. M. H., *Topics Catal.*, in press.
8. Holm, V. C. F., and Bailey, G. C., U.S. Patent 3,032,599 (1962).
9. Hino, M., Kobayashi, S., and Arata, K., *J. Am. Chem. Soc.* **101**, 6439 (1979).
10. Hino, M., and Arata, K., *Chem. Commun.*, 851 (1980).
11. Hsu, C. Y., Heimbuch, C. R., Armes, C. T., and Gates, B. C., *Chem. Commun.*, 1645 (1992).
12. Baba, S., Shibata, Y., Kawamura, T., Takaoka, H., Kimura, T., Kousaka, K., Minato, Y., Yokoyama, N., Lida, K., and Imai, T., Europ. Patent 174836 (1986).
13. Hino, M., and Arata, K., *Chem. Commun.*, 789 (1995).
14. Coelho, M. A., Resasco, D. E., Sikabwe, E. C., and White, R. L., *Catal. Lett.* **32**, 253 (1995).
15. Song, X., Reddy, K. R., and Sayari, A., *J. Catal.* **161**, 206 (1996).
16. Adeeva, V., Lei, G. D., and Sachtler, W. M. H., *Appl. Catal. A* **118**, L11 (1994).
17. Adeeva, V., de Haan, J. W., Jänchen, J., Lei, G. D., Schünemann, V., van de Ven, L. J. M., Sachtler, W. M. H., and van Santen, R. A., *J. Catal.* **151**, 364 (1995).
18. Liu, H., Adeeva, V., Lei, G. D., and Sachtler, W. M. H., *J. Mol. Catal. A: Chemical* **100**, 35 (1995).
19. Liu, H., Lei, G. D., and Sachtler, W. M. H., *Appl. Catal. A: Gen.* **146**, 165 (1996).
20. Hosoi, T., Shimidzu, T., Itoh, S., Baba, S., Takaoka, H., Imai, T., and Yokoyama, N., *Prepr. Am. Chem. Soc. Div. Pet. Chem.* **33**, 562 (1988).
21. Iglesia, E., Soled, S. L., and Kramer, G. M., *J. Catal.* **144**, 238 (1993).
22. Umansky, B., Engelhardt, J., and Hall, W. K., *J. Catal.* **127**, 128 (1991).
23. Babou, F., Courdurier, G., and Vedrine, J. C., *J. Catal.* **152**, 341 (1995).
24. Kustov, L. M., Kazansky, V. B., Figueras, F., and Tichit, D., *J. Catal.* **150**, 143 (1994).
25. Fogash, K. B., Yaluris, G., González, M. R., Ouraipryvan, P., Ward, D. A., Ko, E. I., and Dumesic, J. A., *Catal. Lett.* **32**, 241 (1995).
26. Yaluris, G., Larson, R. B., Kobe, J. M., González, M. R., Fogash, K. B., and Dumesic, J. A., *J. Catal.* **158**, 336 (1996).
27. González, M. R., Kobe, J. M., Fogash, K. B., and Dumesic, J. A., *J. Catal.* **160**, 290 (1996).
28. González, M. R., Fogash, K. B., Kobe, J. M., and Dumesic, J. A., *Catal. Today* **33**, 303 (1997).
29. Armendariz, H., Sanchez Sierra, C., Figueras, F., Coq, B., Mirodatos, C., Lefebvre, F., and Tichit, D., *J. Catal.* **171**, 85 (1997).
30. Cheung, T., d'Itri, J. L., Lange, F. C., and Gates, B. C., *Catal. Lett.* **31**, 153 (1995).
31. Cheung, T. K., d'Itri, J. L., and Gates, B. C., *J. Catal.* **153**, 344 (1995).
32. Karabatsos, G. J., Orzech, C. E., and Meyerson, S., *J. Am. Chem. Soc.* **86**, 1994 (1964).
33. Bearez, C., Avendano, F., Chevalier, F., and Guisnet, M., *Bull. Soc. Chim. France* 346 (1985).
34. Guisnet, M. R., *Acc. Chem. Res.* **23**, 392 (1990).
35. Adeeva, V., Lei, G. D., and Sachtler, W. M. H., *Catal. Lett.* **33**, 135 (1995).
36. Cheung, T. K., d'Itri, J. L., and Gates, B. C., *J. Catal.* **151**, 464 (1995).
37. Zarkalis, A. S., Hsu, C. Y., and Gates, B. C., *Catal. Lett.* **37**, 1 (1996).
38. Zarkalis, A. S., Hsu, C. Y., and Gates, B. C., *Catal. Lett.* **29**, 235 (1994).
39. Fogash, K. B., Larson, R. B., Gonzalez, M. R., Kobe, J. M., and Dumesic, J. A., *J. Catal.* **163**, 138 (1996).
40. Trung Tran, M., Gnep, N. S., Guisnet, M., and Nascimento, P., *Catal. Lett.* **47**, 57 (1997).
41. Tábora, J. E., and Davis, R. J., *J. Catal.* **162**, 125 (1996).
42. Riemer, T., and Knözinger, H., *J. Phys. Chem.* **100**, 6739 (1996).
43. Xu, B. Q., and Sachtler, W. M. H., *J. Catal.* **167**, 224 (1997).
44. Dicko, A., Song, X., Adnot, A., and Sayari, A., *J. Catal.* **150**, 254 (1994).
45. Wan, K. T., Khouw, C. B., and Davis, M. E., *J. Catal.* **158**, 311 (1996).
46. Jatia, A., Chang, C., MacLeod, J. D., Okubo, T., and Davis, M. E., *Catal. Lett.* **25**, 21 (1994).
47. Sikabwe, E. C., Coelho, M. A., Resasco, D. E., and White, R. L., *Catal. Lett.* **34**, 25 (1995).
48. Cheung, T., Lange, F. C., and Gates, B. C., *Catal. Lett.* **34**, 351 (1995).
49. Farcasiu, D., Ghenciu, A., and Li, J. Q., *J. Catal.* **158**, 116 (1996).
50. Fogash, K. B., Hong, Z., Kobe, J. M., and Dumesic, J. A., *Appl. Catal.* (1998).
51. Becke, A. D., *J. Chem. Phys.* **98**, 5648 (1993).
52. "Jaguar v 3.0." Schrodinger, Portland, OR, 1997.
53. Frisch, M. J., Trucks, G. W., Schlegel, H. B., Gill, P. M. W., Johnson, B. G., Robb, M. A., Cheeseman, J. R., Keith, T., Petersson, G. A., Montgomery, J. A., Raghavachari, K., Al-Laham, M. A., Zakrzewski, V. G., Ortiz, J. V., Foresman, J. B., Cioslowski, J., Stefanov, B. B., Nanayakkara, A., Challacombe, M., Peng, C. Y., Ayala, P. Y., Chen, W., Wong, M. W., Andres, J. L., Replogle, E. S., Gomperts, R., Martin, R. L., Fox, D. J., Binkley, J. S., Defrees, D. J., Baker, J., Stewart, J. P., Head-Gordon, M., Gonzalez, C., and J. A. Pople, J. A., "Gaussian 94 (Revision C.2)." Gaussian, Pittsburgh, PA, 1995.
54. Hay, P. J., and Wadt, W. R., *J. Chem. Phys.* **98**, 5648 (1985).
55. Jin, T., Yamaguchi, T., and Tanabe, K., *J. Phys. Chem.* **90**, 4794 (1986).
56. Bensitel, M., Saur, O., Lavalley, J. C., and Morrow, B. A., *Mater. Chem. Phys.* **19**, 147 (1988).
57. Riemer, T., Spielbauer, D., Hunger, M., Mekhemer, G. A. H., and Knözinger, H., *Chem. Commun.*, 1181 (1994).
58. Clearfield, A., Serrette, G. P. D., and Khazi-Syed, A. H., *Catal. Today* **20**, 295 (1994).
59. White, R. L., Sikabwe, E. C., Coelho, M. A., and Resasco, D. E., *J. Catal.* **157**, 755 (1995).

60. Bearez, C., Chevalier, F., and Guisnet, M., *React. Kinet. Catal. Lett.* **22**, 405 (1983).
61. Garin, F., Andriamasinoro, D., Abdulsamad, A., and Sommer, J., *J. Catal.* **131**, 199 (1991).
62. Garin, F., Seyfried, L., Girard, P., Maire, G., Abdulsamad, A., and Sommer, J., *J. Catal.* **151**, 26 (1995).
63. Tábora, J. E., and Davis, R. J., *J. Am. Chem. Soc.* **118**, 12240 (1996).
64. Farcasiu, D., "214th National Meeting, Amer. Chem. Soc., Las Vegas, NV, Sept., 1997, 1997," p. 745.
65. Farcasiu, D., Ghenciu, A., and Miller, G., *J. Catal.* **134**, 118 (1992).
66. Farcasiu, D., and Ghenciu, A., *Progr. NMR Spectro.* **29**, 129 (1996).
67. Ng, F. T. T., and Horvát, N., *Appl. Catal. A:Gen* **123**, L197 (1995).
68. Okuhara, T., Nishimura, T., Watanabe, H., and Misono, M., *J. Mol. Catal.* **74**, 247 (1992).
69. Olah, G. A., and Molnar, A., *in* "Hydrocarbon Chemistry," Wiley, New York, 1995.
70. Fogash, K. B., Hong, Z., and Dumesic, J. A., *J. Catal.* **173**, 519 (1998).
71. Olah, G. A., *Angew. Chem. Int. Ed. in English* **12**, 173 (1973).
72. Brouwer, D. M., and Hogeveen, H., "PROGRESS, in Progress in Physical Organic Chemistry" (A. J. Streitwieser and R. W. Taft, Eds.), p. 179. Wiley, New York, 1972.
73. Brouwer, D. M., *in* "NATO, in Chemistry and Chemical Engineering of Catalytic Processes" (R. Prins and G. C. A. Schuit, Eds.), p. 137. Sijthoff & Noordhoff, Alphen a/d Rijn, 1980.
74. Kondo, J., Skata, Y., Domen, K., Maruya, K., and Onishi, T., *J. Chem. Soc., Faraday Trans.* **86**, 397 (1990).
75. Onishi, T., Abe, H., Maruya, K., and Domen, K., *Chem. Commun.*, 617 (1985).
76. Nakatsuji, H., Hada, M., Ogawa, H., Nagata, K., and Domen, K., *J. Phys. Chem.* **98**, 11840 (1994).
77. Kokes, R. J., and Dent, A. L., *Adv. Catal.* **22**, 1 (1972).
78. Domen, K., Kondo, J., Maruya, K., and Onishi, T., *Catal. Lett.* **12**, 127 (1992).
79. Kobe, J. M., González, M. R., Fogash, K. B., and Dumesic, J. A., *J. Catal.* **164**, 459 (1996).